POLISH MARITIME RESEARCH Special Issue 2017 S3 (95) 2017 Vol. 24; pp. 235-242
10.1515/pomr-2017-0128

# IDENTIFICATION ALGORITHM OF UNCERTAIN SONAR SIGNALS IN COMPLEX MARINE ENVIRONMENT

**Xuefeng Zhang**
School of Information and Communication Engineering, North University of China, Taiyuan 030051, China

**ABSTRACT**

*The current identification algorithm using sonar signal parameters of bandwidth, frequency, duration and pulse waveform which are easy to detect and imitation, to identify the identity of sonar signal, resulting in part of the sonar signal identity is not easy to distinguish. Therefore, an algorithm based on signal feature extraction and digital watermarking is proposed to recognize the uncertain sonar signals. The algorithm embeds the digital watermark into the detection signal from the uncertain sonar. The identity of the signal is recognized by detecting whether the received signal contains watermarks. Experimental results showed that the proposed algorithm can effectively improve the recognition performance of sonar signal source.*

**Keywords:** Complex marine environment; Uncertain sonar signals; Identification algorithms

## INTRODUCTION

The ocean contains huge resources and benefits, making it gradually become a hot spot in the world. Therefore, understanding of underwater conditions becomes particularly important [1-2]. As an effective means of underwater detection and communication, underwater acoustic signals have been paid more and more attention by people [3]. With the development of underwater detection and communication technology, the marine environment is filled with many sound signals, the enemy often launch with highly similar signal which identity are not easy to distinguish to implement interference or trick [4]. Therefore, how to determine the identity of received underwater acoustic signals has become an urgent problem that needs to be solved [5]. The existing sonar signal identification algorithm uses sonar parameters such as bandwidth, frequency, duration and pulse waveform which are easy to detect and imitate, resulting in part of the sonar signal identity is not easy to distinguish [6]. Therefore, a new identification algorithm of uncertain sonar signals in complex marine environment is proposed. In the sonar signal, digital watermark is embedded, the identity of the signal is recognized by detecting whether the received signal contains watermarks.

## IDENTIFICATION ALGORITHM OF UNCERTAIN SONAR SIGNALS IN COMPLEX MARINE ENVIRONMENT

### A. ANALYSIS OF UNCERTAIN SONAR SIGNALS IN COMPLEX MARINE ENVIRONMENT

In complex marine environment, different signal waveforms will produce different processing results and different detection performance. Wavelet analysis theory is used to extract the energy features of different sonar signals in complex marine environment. Hilbert spectrum features

of uncertain sonar signals are extracted by Hilbert Huang transform method [7]. Different types of sonar signal features are extracted by several algorithms. The specific process is as follows:

(1) energy extraction in different frequency bands based on wavelet packet decomposition

Taking the three-level wavelet packet decomposition as an example, the wavelet packet decomposition algorithm and the steps of extracting the energy features in each frequency band of the uncertain sonar signals in complex marine environment are given. The structure of the three-layer wavelet packet decomposition is shown in figure 1.

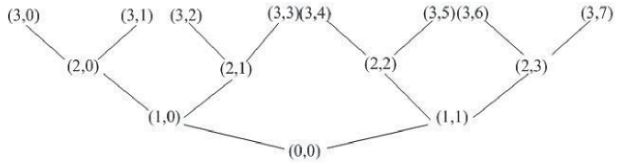


*Fig. 1. Structure Diagram of Three-layer Wavelet Packet Decomposition*

$(i, j)$ represents the $j$ node in the $i$ layer, $i = 0,1,2,3$, $j = 0,1,2,3,\cdots,7$, each node represents a certain feature of sonar signal, where(0,0) represents the original signal *S*; (1,0) represents the low frequency coefficient $X_{10}$ of first layer in wavelet packet decomposition; (1,1) represents the high frequency coefficient $X_{10}$ of first layer in wavelet packet decomposition, in order to push.

The first step: in the complex marine environment, the original sonar signal is carried out with three-layer wavelet packet decomposition;

The second step: the wavelet signal decomposition is used to reconstruct the sonar signal, and obtained the reconstructed signal in each frequency band of the sonar signal.

$$S = S_{30} + S_{31} + \cdots + S_{37} \tag{1}$$

Where $S_{ij}$ represents the reconstruction signal corresponding to $X_{ij}$.

Assumed that in a complex marine environment, the minimum frequency component of an uncertain sonar signal is 0, and the highest frequency component is 1. The frequency ranges they represent each are shown in Table 1.

*Tab. 1. The Frequency Range Represented by the Reconstructed Signal*

| Uncertain sonar signal | Frequency range /Hz | Uncertain sonar signal | Frequency range /Hz |
|---|---|---|---|
| S30 | 0-0.125 | S34 | 0.500-0.625 |
| S31 | 0.125-0.250 | S35 | 0.625-0.750 |
| S32 | 0.250-0.375 | S36 | 0.750-0.875 |
| S33 | 0.375-0.500 | S37 | 0.875-1.000 |

The third step: to find the energy $E_j (j = 0,\cdots,7)$ of the reconstructed signals in the frequency bands of the uncertain sonar signals, $E_j = \sqrt{\sum_{k=1}^{K} \left| S_{3j}(k) \right|^2}$, $S_{3j}(k)$ represents the magnitude of the discrete points of the reconstructed signal $S_{3j}$, $k = 1,2,\cdots,N$ and $N$ are the points of the reconstructed signals.

The fourth step: construct the feature vector of uncertain sonar signals. $E_j$ represents the energy of the reconstructed signal, with a total energy of $E = \sqrt{\sum_{j=0}^{7} E_j^2}$. The feature quantity is $F$:

$$F = \left[ \frac{E_0}{E}, \cdots, \frac{E_7}{E} \right] \tag{2}$$

According to the frequency range represented by the decomposed signal, the feature vectors extracted from the first class of sonar signals by wavelet packet decomposition can well represent the feature information of the target signals.

(2) Hilbert spectrum feature extraction based on Hilbert Huang Transform

To study the variation of frequency of uncertain sonar signals with time in complex marine environment, the instantaneous frequency is proposed. There has been a lot of controversies over the definition of instantaneous frequency, until the Hilbert transform and analytic signal method proposed. For any time series $x(t)$ satisfying the requirement, the corresponding Hilbert transform $y(t)$ can be expressed as a lower form:

$$y(t) = \frac{1}{\pi} \int_{-\infty}^{+\infty} \frac{x(\tau)}{t - \tau} d\tau = x(t) * \frac{1}{\pi t} \tag{3}$$

Then we can define the complex analytic signal $x(t)$ of the uncertain sonar signal $z(t)$:

$$z(t) = x(t) + jy(t) = a(t) e^{-j\theta(\tau)} \tag{4}$$

The instantaneous amplitude and instantaneous phase of the sonar signal $z(t)$ are analyzed:

$$a(t) = \sqrt{x^2(t) + y^2(t)} \tag{5}$$

$$\theta(t) = \arctan \frac{y(t)}{x(t)} \tag{6}$$

The instantaneous frequency of an uncertain sonar signal $x(t)$ is defined as:

$$w(t) = \arctan \frac{d\theta(t)}{d(t)} \tag{7}$$

The instantaneous frequency of an uncertain sonar signal in a complex marine environment is the angular frequency of the signal at a moment, or it can be regarded as instantaneous phase change rate over time.

For stationary sonar signals, an analytic sonar signal with physical significance can be obtained by using the

instantaneous frequency defined above which solves the problem of negative frequency after Fourier transformation. But for non-stationary signals in the uncertain sonar signal, the frequency changes over time. The instantaneous frequency obtained after the direct Hilbert transform can also be negative which has no physical meaning. To solve this problem, empirical mode decomposition [8] is adopted to deal with the problem:

The first step: find out the extremum points of the original sonar signal $x(t)$, that is, the maximum and minimum points. The upper and lower envelopes of extreme points are obtained through the method of interpolation fitting;

The second step: calculate the mean value of the upper and lower envelope of the extremum point, denoted as $m_{10}(t)$.

The third step: calculate the difference between $x(t)$ and $m_{10}(t)$, which is denoted as $h_{10}(t)$.

$$h_{11}(t) = h_{10}(t) - m_{11}(t) \tag{8}$$

The fourth step: verify that if $h_{10}(t)$ meets the requirements of IMF. If satisfied, make $imf1 = h_{10}(t)$; otherwise, take $h_{10}(t)$ as a new signal sequence, in accordance with step 1 to 3, get the upper and lower envelope mean $m_{11}(t)$, and calculate the difference between $h_{10}(t)$ and $m_{11}(t)$, denoted as $h_{11}(t)$:

$$h_{11}(t) = h_{10}(t) - m_{11}(t) \tag{9}$$

The fifth step: verify that if $h_{11}(t)$ meets the IMF requirement. Repeat the operation several times until $h_{1i}(t)$ meets the IMF requirement. So far, the signal $imf_1(t)$ has been received;

$$imf_1 = h_{1i}(t) \tag{10}$$

The sixth step: separate $imf_1(t)$ from the original uncertainty sonar signal $x(t)$ and get the signal $r_1(t)$:

$$r_1(t) = x(t) - imf_1(t) \tag{11}$$

The seventh step: take $r_1(t)$ as a new signal sequence and repeat the above steps to find the other IMF components;

The eighth step: get a margin $r_n(t)$ that hat can no longer be decomposed by EMD, which is called the residual component;

At this time, the original sonar signal $x(t)$ can be expressed as a sum of finite intrinsic modes and functions after EMD decomposition.

$$x(t) = \sum_{i=1}^{n} imf_i(t) + r_n(t) \tag{12}$$

After EMD decomposition, in complex marine environment, the uncertainty sonar signals can be expressed as the sum of multiple IMF components and residuals. The residual of a sonar signal represents a long-period oscillation, either a constant or a monotonic function, which may contain great energy. Therefore, in practical applications, according to the needs of the study to decide whether to retain. The definition of the instantaneous frequency and the instantaneous phase in front can be obtained, and each IMF can be expressed as:

$$imf_i(t) = \mathrm{Re}((a_i(t)\exp(j\theta_i(t))) = \mathrm{Re}(a_i(t)\exp(j\int \omega_i(t)dt)) \tag{13}$$

Then the original uncertainty sonar signal $x(t)$ can be represented as:

$$x(t) = \mathrm{Re}(\sum_{i=1}^{n} a_i(t)\exp(j\int \omega_i(t)dt)) \tag{14}$$

Then we can do the Hilbert transform for each IMF component to obtain its instantaneous amplitude and instantaneous frequency, and summarize the instantaneous amplitude and instantaneous frequency of all IMF. Hilbert marginal spectrum is the total amplitude of instantaneous frequency of uncertain sonar signals in complex marine environment, which reflects the amplitude distribution at each frequency point.

Suppose there is a marine sonar signal with a sampling point of $N$, the sampling frequency is $f_s$, and the time length is $T$. According to Fourier analysis theory, the highest frequency component of the Fourier transform signal is $f_s/2$, and the frequency resolution of marine sonar signal is fixed $f_s/N$. By the theory of Hilbert transform [9], the frequency of the Hilbert marginal spectrum [10] is the instantaneous frequency, and is the derivative of the phase of its corresponding analytic signal. The highest instantaneous frequency of the Hilbert spectrum of marine sonar signals is the highest frequency inherent to the sampled signals. The frequency resolution in the Hilbert marginal spectrum is related to the sampling number N and the highest frequency inherent to the marine sonar signal:

$$\Delta f = f_{\max} / N \tag{15}$$

Due to the advantage of Hilbert marginal spectrum relative to Fourier amplitude spectrum and its higher frequency resolution, we use the HHT method to extract the marginal spectral features of the uncertain sonar signals in complex marine environment.

## B. DETECTION OF UNCERTAIN SONAR SIGNAL

The processing structure of the sonar signal receiver primarily depends on the form of the transmitted signal, the sonar signal processing has been smoothly smooth to obtain the smoothing weight coefficient and steady signal, the received signal is defined:

$$x(n)' = s(n)' + n(n)' \tag{16}$$

Where, $s(n)'$ is the target echo signal, $n(n)'$ and $(0,\sigma^2)$ is the distributed Gauss white noise, and the signal is not correlated with noise.

In complex marine environment, the conditional probability density of the unknown sonar signal detection statistic $M$ is:

$$p(M/H_1)=\frac{M}{\sigma^2}\exp(-\frac{M^2+(aN/2^2)}{2\sigma^2})I_0(\frac{MaN}{2\sigma^2}) \quad (17)$$

$$p(M/H_0)=\frac{M}{\sigma^2}\exp(-\frac{M^2}{2\sigma^2}) \quad (18)$$

Formulae (17) and formulae (18) are Rician and Rayleigh distributions, where $a$ is the amplitude of sonar signals. Thus, the false alarm probability is:

$$P_F=\exp(-\frac{\lambda^2}{2\sigma^2}) \quad (19)$$

The detection probability is:

$$P_D=\int_\lambda^\infty \frac{M}{\sigma^2}\exp(-\frac{M^2+(aN/2)^2}{2\sigma^2})I_0(\frac{MaN}{2\sigma^2})dM \quad (20)$$

Formulae (16) to (20) determines the detection performance of the receiver of uncertain sonar signals in complex marine environment.

## C. MATHEMATICAL WATERMARKING MODEL FOR UNDERWATER ACOUSTIC CHANNEL IN COMPLEX MARINE ENVIRONMENT

In the complex marine environment, if the velocity distribution function of underwater acoustic channel is $c(z)$, the position of the point source is $(r_0,z_0)$, and the initial sound velocity is $c_0$. Then, the sound propagation track $r$ and propagation time $t$ of any point source $(r,z)$ with an initial grazing $\theta_0$ at any point on the acoustic line of the initial grazing can be expressed in the lower form:

$$r=r_0+\int_{z_0}^{z}\frac{\cos\theta_0}{\sqrt{n^2-\cos^2\theta_0}}dz \quad (21)$$

$$r=\frac{1}{c_0}\int_{z_0}^{z}\frac{n^2(z)}{\sqrt{n^2-\cos^2\theta_0}}dz \quad (22)$$

Where, $n(z)=c_0/c(z)$ represents refractive index.

In complex marine environment, the geometric propagation loss between the sound source and the receiving point can be calculated by the cross-sectional area of the acoustic beam tube between the two adjacent sound sources, as shown in figure 2.

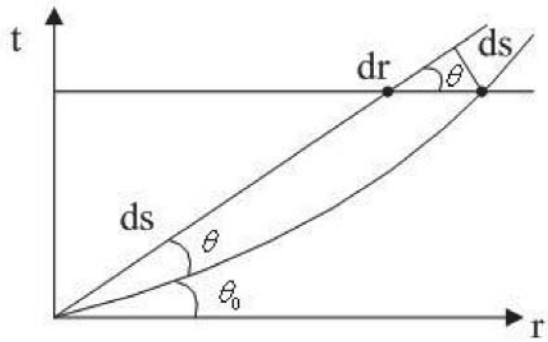


*Fig. 2. The Propagation of Sound Energy Along the Ray Tube Bundle*

Considering two acoustic lines emitted by the acoustic source at grazing angle $\theta_0$ and $\theta_0+d\theta_0$, they propagate along the acoustic track in the marine and arrive near the receiving point. The horizontal distance is $dr$. In $d\theta_0$, the sound power radiated from the sound source is $\Delta P$. According to the physical meaning of the sound intensity equation, the sound power between the sound lines is the same at the receiving point. In the sound beam tube, the sound intensity at the unit distance is $I_0$, the vertical area of the sound line is:

$$dS_0=2\pi\cos\theta_0 d\theta_0 \quad (23)$$

At the receiving point $(r,z)$, the vertical area of the sound line is:

$$dS=2\pi r\sin\theta dr \quad (24)$$

At the receiving point $(r,z)$,the sound intensity $I$ and the sound pressure $A$ is:

$$I=\frac{I_0\cdot dS_0}{dS}=\frac{I_0\cos\theta d\theta_0}{r\cdot\cos\theta dr} \quad (25)$$

$$A=\sqrt{I} \quad (26)$$

The impulse response function $h(t)$ of multipath channels can be determined by calculating the intrinsic sound line parameters:

$$h(t)=\sum_{i=1}^{N}A_i\delta(t-t_i) \quad (27)$$

$$A_i=(-1)^N\cdot\frac{\sqrt{I_i}}{\sqrt{I_{\max}}} \quad (28)$$

$$\tau_i=t_i-t_{\min} \quad (29)$$

Where $N$ represents the total number of active channels in the sound field, $A_i$ represents the normalized sound pressure amplitude value of a propagation path of the original sound, $I_i$ represents the sound pressure amplitude value, $I_{\max}$ represents the maximum amplitude of sound pressure, $\tau_i$ represents relative delay, $t_i$ represents the delay and $t_{\min}$ represents the minimum delay.

If the transmit signal is $s(t)$, then the received signal is $y(t)$:

$$y(t)=s(t)*h(t)=s(t)*\left[\sum_{i=1}^{n}A_i\delta(t-t_i)\right] \quad (30)$$

If the transmit signal 1 meter from the sound source is $s(t)$, then the received signal is $y(t)$, and the transmission loss is $TL$:

$$TL=101g\frac{\frac{1}{T}\int_0^T s^2(t)dt}{\frac{1}{T}\int_0^T y^2(t)dt}=101g\frac{\frac{1}{T}\int_0^T s^2(t)dt}{\frac{1}{T}\int_0^T\left[\sum_{i=1}^{N}A_i s(t-\tau_i)\right]^2dt} \quad (31)$$

The watermark $W$ generated by the watermark generation algorithm is generally related to the key $K$ and the secret information $m$, but in some applications, the watermark information is also related to the carrier content, the sonar signal $S$. Therefore, $W = W(K, m)$, after the watermark embedding algorithm, the watermark is embedded into the sonar signal $S$ is the watermarked signal $S_W$ can be expressed as $S_W = T(W, S)$. The received watermarked signal $S'_W$ is transmitted via the underwater acoustic channel H from the watermarked signal $S_W$ which can be expressed as $S'_W = H(S_W)$. Using the watermark extraction, detection algorithm $D$ and watermark template $W$ on the received watermark signal $S'_W$, considering the marine channel and additional noise in the channel, assuming the received signal can be expressed as $r_{w0}$:

$$r_{w0} = s_w * h + n_0 = s'_w + n_0 \tag{32}$$

Where $h$ represents the impulse response of marine channel, and $n_0$ represents an additive noise in the channel. Due to the influence of the ocean channel there will be a multi-way effect, the received signal will be extended in the time domain. In watermark detection, the same part of $r_w$ as long as $s$ is still taken from $r_{w0}$. On this basis, the received watermark signal $r_w$ is performed three-layer DWT transform, and then the low frequency sub-band is transformed by DCT. Finally, according to the watermark length and the embedded position, it can be obtained:

$$R_w = dwt(r_w) = (R_1, \cdots, R_4) \tag{33}$$

In the formula, $R_w$ represents the wavelet coefficients of $r_w$ after three-layer wavelet transform.

$$S'_{1Dw} = dwt(R_1) = (s'_{1DW}, \cdots, s'_{\frac{n}{8}DW}) \tag{34}$$

As shown in equation (34), $S'_{1Dw}$ is the coefficient embedded in the watermark.

## EXPERIMENTAL RESULTS AND ANALYSIS

In this experiment, the actual marine test data of a kind of towed line array sonar is used as the verification of the identification algorithm of the sonar signal and each of the experimental tests obtained the sonar signal as a sample, a total of 50 sample data are obtained as a random signal of multiple different appearances. The experiment completed on the Matlab platform, compared the proposed algorithm with the matched filter detection algorithm, the validity of the proposed algorithm is verified by two aspects of the uncertain sonar signal detection result and the watermarked sonar signal detection result.

### A. DETECTION AND ANALYSIS OF UNCERTAIN SONAR SIGNALS

Figure 3 (a) showed the towed array sonar signal, the transmit signal bandwidth in the experiment is 30kHz, pulse width is 3.0ms, the center frequency is 30kHz; the sampling frequency is 100 kHz; the target echo located in 13.0 to 15.5ms, reverberation ratio is -1.0dB. The uncertain sonar signals are smoothed to obtain the weighting factor and the signal after the stabilization, as shown in Figure 3 (b) and figure 3 (c), respectively. To compare with the matched filtering method, the smoothing reverberation is first matched and filtered, and the result is shown in Figure 3 (d). Figure3 (e) is the output of the signal detection in the proposed method.

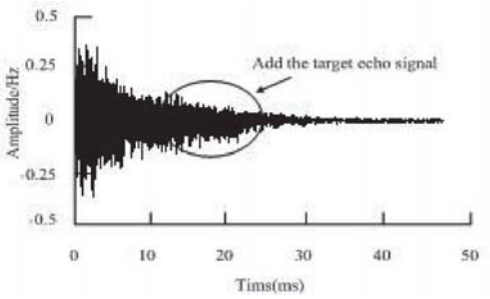


*(a) Uncertain Signals in Simulation Marine Environment*

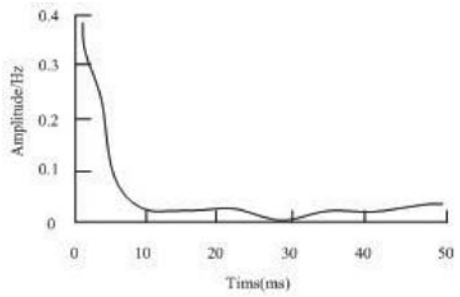


*(b) Weight Coefficient*

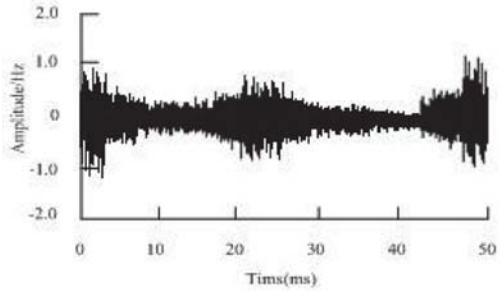


*(c) Smooth Reverberation*

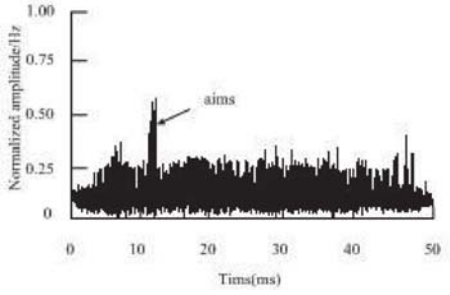


*(d) Matched Filtered Output*

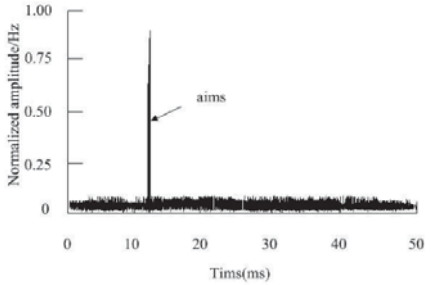


*(e) Filter Output in This Paper*

*Fig. 3. Data Processing Results of Sea Trial Test*

Figure 3 (e) showed that the proposed method can suppress the reverberation noise, detect the position of the target echo signal, and the has a better ability to suppress the reverberation than the matched filtering method [11-12].

The Monte Carlo method was used to calculate the experimental results to obtain the Receiver operating characteristic(ROC) curve of the experimental receiver. The ROC curve showed that under the condition of a fixed signal mixing ratio, different threshold values correspond to different detection probability and false alarm probability [13-15]. By using the proposed algorithm and the matched filter detection algorithm on sea trial data processing, for the signal containing the target, in a fixed threshold, if the detection output is greater than the threshold, the target is detected, otherwise is not, which can estimate the detection probability of the threshold. Figure 4 showed the ROC curve at the signal mixing ratio of -2.0dB. The dotted line is the ROC curve of the matched filter detector, and the solid line is the ROC curve of the proposed algorithm. Figure 5 showed the ROC curve of the sea trial results, with a mixing ratio of 4.5dB. In the complex marine environment, the signal mixture ratio is not easy to measure [16]. The signal mixture ratio is obtained by formula (35):

$$SRR = 10\log(\frac{P_{s+r} - P_r}{P_r}) \quad (35)$$

Where, $SRR$ is the signal mixture ratio; $P_{s+r}$ is the signal power of the target echo signal position which contains two parts of the target echo signal and the reverberation signal; $P_r$ is the reverberation signal power near the target echo signal. $P_r$ is used to approximate the reverberation signal power contained in the target echo signal location.

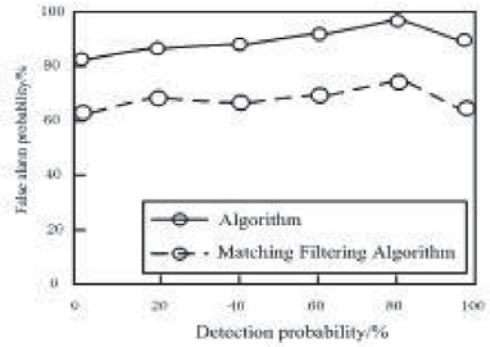


*Fig. 4. ROC Curve under Simulated Signal SRR of -2.0dB*

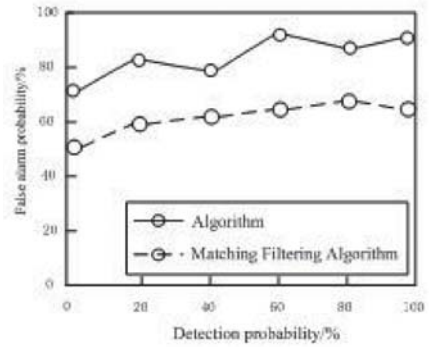


*Fig. 5. ROC Curve under Sea Trial Signal SRR of 4.5dB*

Figure 4 and figure 5 showed that the detection performance of the proposed method is superior to that of the matched filter. It is also found that the signal mixture ratio of simulation signal is less than the sea test signal, but the simulation signal performance is better, this is because the sea trial data contains strong interference signal, thus increasing the probability of false alarm. The stability of reverberation also affect the detection performance [17]. In the data processing, it is found that the unreasonable stabilization method can also reduce the detection performance [18].

## B. DETECTION AND ANALYSIS OF WATERMARKED SONAR SIGNALS

To verify the effectiveness and performance of the proposed algorithm, the detection performance of the watermarked sonar signal is analyzed.

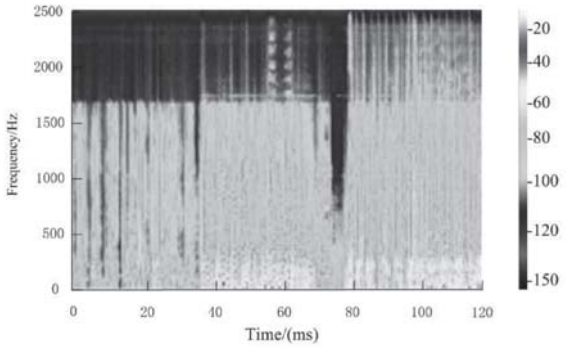


*(a) Original Carrier Signal*

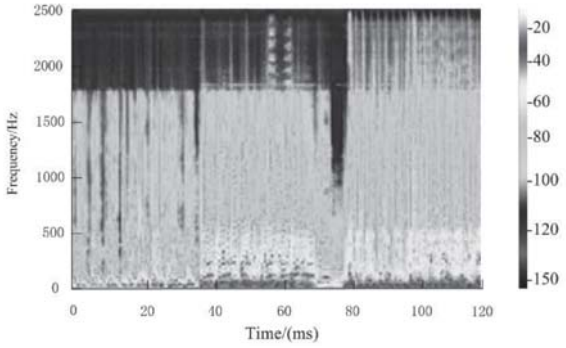


*(b) Watermarked Signals (noiseless)*

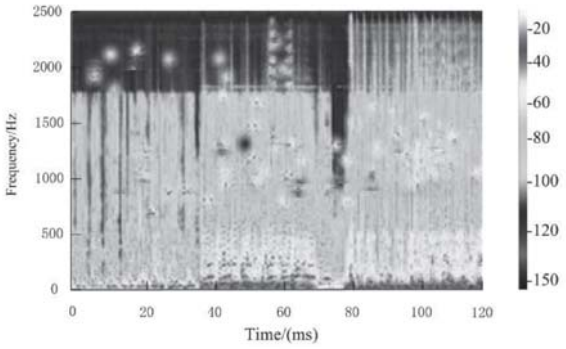


*(c) Watermarked Signal (SNR=20dB)*

*Fig 6. Signal Analysis Spectrum*

Figure 6 showed the spectrums of original signal, the watermarked signal (noiseless) and the watermarked signal (SNR=20dB), combined with the results shown in Figure 1, table 2 gives the specific performance of the watermark detection under different SWR conditions.

*Tab. 2. Watermark Detection Results under Different SWR Conditions*

| Watermark embedding ratio | The false alarm probability /% | The probability of missed/% |
|---|---|---|
| SWR=30dB | 1.09 | 0.7 |
| SWR=45dB | 4.9 | 2.7 |
| SWR=60dB | 7.0 | 3.6 |
| SWR=75dB | 9.4 | 4.8 |

Figure 6 and table 2 showed that with the increase of SWR, the probability of false alarm and the failure probability increases gradually, but the false alarm probability and failure probability of the proposed method are not high, which proved that this method has a better detection performance of watermarking.

## RESULTS AND DISCUSSION

For the difficulty to identify the identity of the received signal for the uncertainty in the complex marine environment, it is proposed to embed digital watermark in the active sonar transmit signal and detect whether the received signal contains the embedded watermark, and then realize the identity of uncertain sonar signals.

The main results of this paper are as follows:

1. The features of uncertain sonar signals and signal detection in complex marine environment are systematically studied and analyzed. A method of sonar identification using digital watermarking technology is proposed, and the feasibility and performance of this method are analyzed combined with sonar signal detection and detection resolution.
2. Underwater acoustic channel model is established based on the eigen ray model of, and digital watermarking model of underwater acoustic channel is established based on this model. Simulation results showed that the Influence of underwater acoustic channel on watermarking should be considered in the design of watermarking algorithm.
3. Considering the coherence of underwater acoustic channel, a block based DCT watermarking algorithm is designed and implemented. Firstly, the original carrier signal is partitioned according to the features of the underwater acoustic channel, and then the DCT transform is used for each sub-block. Finally, the watermark is embedded into each sub-block. The normalized correlation value is proposed at the end of the detection, so that the correlation value can be independent of the signal amplitude, which can improve the detection rate. Through simulation analysis, the feasibility and security of the algorithm are verified, and the shortcomings of this method are also proposed.

Through simulation analysis, it is proved that the proposed algorithm can improve watermark detection rate and signal resolution performance in the case of no significant impact on the detection performance of the sonar signal. Therefore, the research of this subject has great significance and practical value.

## REFERENCES

1. Ferguson B G, Lo K W. Passive and active sonar signal processing methods for port infrastructure protection and harbor security. Journal of the Acoustical Society of America, 2016, 140(4):3350-3350.

2. Wei C, Wwl A, Ketten D R, et al. Biosonar signal propagation in the harbor porpoise's (Phocoena phocoena) head: The role of various structures in the formation of the vertical beam.. Journal of the Acoustical Society of America, 2017, 141(6):4179.

3. Au W W, Copeland A, Martin S W, et al. Comparing the biosonar signals of free swimming dolphins with those of a stationary dolphin in a net pen. Journal of the Acoustical Society of America, 2015, 137(4):2335-2335.

4. Parks J K. Development of a Multichannel Optical Correlation Detector for Sonar Signals. Journal of Aircraft, 2015, 3(3):278-284.

5. Au W W L, Martin S W, Moore P W, et al. Dynamics of biosonar signals in free-swimming and stationary dolphins: The role of source levels on the characteristics of the signals. Journal of the Acoustical Society of America, 2016, 139(3):1381-1389.

6. De Maio A, Orlando D, Hao C, et al. Adaptive Detection of Point-Like Targets in Spectrally Symmetric Interference. IEEE Transactions on Signal Processing, 2016, 64(12):3207-3220.

7. Scandella B P, Pillsbury L, Weber T, et al. Ephemerality of discrete methane vents in lake sediments. Geophysical Research Letters, 2016, 43(9):n/a-n/a.

8. Wei C, Wwl A, Ketten D R, et al. Biosonar signal propagation in the harbor porpoise's (Phocoena phocoena) head: The role of various structures in the formation of the vertical beam.. Journal of the Acoustical Society of America, 2017, 141(6):4179.

9. Au W W, Copeland A, Martin S W, et al. Comparing the biosonar signals of free swimming dolphins with those of a stationary dolphin in a net pen. Journal of the Acoustical Society of America, 2015, 137(4):2335-2335.

10. LIANG Wei-xin，FENG Yong-xin，QIAN Bo，et al.An Optimization Recognition Algorithm of Amplitude-Frequency Modulation Signals. Computer Simulation, 2016，33(8):415-420.

11. Gao, W. and W. Wang, The fifth geometric-arithmetic index of bridge graph and carbon nanocones. Journal of Difference Equations and Applications, 2017. 23(1-2SI): p. 100-109.

12. Gao, W., et al., Distance learning techniques for ontology similarity measuring and ontology mapping. Cluster Computing-The Journal of Networks Software Tools and Applications, 2017. 20(2SI): p. 959-968.

13. De'nan F, Nazri F M, Hashim N S. Finite Element Analysis on Lateral Torsional Buckling Behaviour Oi I-Beam with Web Opening. Engineering Heritage Journal, 2017, 1(2):19–22.

14. Sarkar M I, Islam M N, Jahan A, Islam A, Biswas J C. Rice straw as a source of potassium for wetland rice cultivation. Geology, Ecology, and Landscapes, 2017, 1(3): 184-189.

15. Foroozanfar M. Environmental control in petroleum operations. Journal CleanWAS, 2017, 1(2): 18-22.

16. Wang J, Xu H. The Crust and Uppermost Mantle S-Wave Velocity Structure Beneath Japan Islands Revealed by Joint Analysis of P - And SWave Receiver Functions. Malaysian Journal Geosciences, 2017, 1(2): 20-23.

17. Tahir S, Siong K Y, Musta B, Asis J. Facies and Sandstone Characteristics of The Kudat Formation, Sabah, Malaysia. Geological Behavior, 2017, 1(2):20–25.

18. Shamsudin S B, Majid A A. Association of blood lead levels and working memory ability of primary school children surrounding ex-copper mining area in Ranau, Sabah (Malaysia). Acta Scientifica Malaysia, 2017, 1(1): 01-03.

**CONTACT WITH THE AUTHOR**

Xuefeng Zhang

*e-mail: wmsgczyz@163.com*

School of Information and Communication Engineering
North University of China
Taiyuan 030051
**CHINA**